Preprints.org

Article

Not peer-reviewed version

Characterization of Novel and Known Activators of Cannabinoid Receptor Subtype 2 Reveals Mixed Pharmacology that Differentiates Mycophenolate Mofetil and GW-842,166X from MDA7

Alice L. Rodriguez , Aidong Qi , Allie Han , Haley E. Kling , Marc C. Quitalig , Aaron M. Bender , Lisa Barbaro , David Whomble , Craig W. Lindsley , Colleen M. Niswender *

Posted Date: 22 April 2025

doi: 10.20944/preprints202504.1842.v1

Keywords: cannabinoid receptor; allosteric modulator; mycophenolate mofetil; GW-842,166X; MDA7; brain disorders

Preprints.org is a free multidisciplinary platform providing preprint service that is dedicated to making early versions of research outputs permanently available and citable. Preprints posted at Preprints.org appear in Web of Science, Crossref, Google Scholar, Scilit, Europe PMC.

Copyright: This open access article is published under a Creative Commons CC BY 4.0 license, which permit the free download, distribution, and reuse, provided that the author and preprint are cited in any reuse.

Preprints.org (www.preprints.org) | NOT PEER-REVIEWED | Posted: 22 April 2025 doi:10.20944/preprints202504.1842.v1

Disclaimer/Publisher's Note: The statements, opinions, and data contained in all publications are solely those of the individual author(s) and contributor(s) and not of MDPI and/or the editor(s). MDPI and/or the editor(s) disclaim responsibility for any injury to people or property resulting from any ideas, methods, instructions, or products referred to in the content.

Article

Characterization of Novel and Known Activators of Cannabinoid Receptor Subtype 2 Reveals Mixed Pharmacology that Differentiates Mycophenolate Mofetil and GW-842,166X from MDA7

Alice L. Rodriguez [1,2], Aidong Qi [1,2], Allie Han [1,2], Haley E. Kling [1,2], Marc C. Quitalig [1,2], Aaron M. Bender [1,2], Lisa Barbaro [1,2], David Whomble [1,2], Craig W. Lindsley [1,2,6] and Colleen M. Niswender [1,2,3,4,5,*]

[1] Warren Center for Neuroscience Drug Discovery, Vanderbilt University, Nashville, TN 37232, USA
[2] Department of Pharmacology, Vanderbilt University School of Medicine, Nashville, TN 37232, USA
[3] Vanderbilt Institute of Chemical Biology, Vanderbilt University, Nashville, TN 37232, USA
[4] Vanderbilt Brain Institute, Vanderbilt University, Nashville, TN 37232, USA
[5] Vanderbilt Kennedy Center, Vanderbilt University Medical Center, Nashville, TN 37232, USA
[6] Department of Chemistry, Vanderbilt University, Nashville TN 37232, USA
* Correspondence: colleen.niswender@vanderbilt.edu; Tel: 615-343-4303

Abstract: CB_1 and CB_2 cannabinoid receptors are members of the GPCR superfamily that modulate the effects of endocannabinoids. CB_1 is the most abundant CB receptor in the central nervous system while CB_2 is present both peripherally and in the brain. CB_2 plays a role in inflammation as well as neurodegenerative and psychiatric disorders. To identify new ligands for CB_2, we screened a library of FDA-approved drugs for activity at the receptor using a thallium flux assay, resulting in the discovery of the immunosuppressant mycophenolate mofetil as a potent, selective activator of CB_2. Further characterization of the compound confirmed agonist activity in a variety of complementary assays including PI hydrolysis, cAMP inhibition, and β-arrestin recruitment. Radioligand binding assays established a non-competitive interaction with the site occupied by [^{3}H]CP55,940. CB_2 agonists GW-842,166X and MDA7 were also profiled, revealing that GW-842,166X exhibits a similar activity profile to mycophenolate mofetil, whereas MDA7 presents a distinct profile. These differences provide insight into the complicated CB_2 pharmacology impacting preclinical and clinical studies and ultimately new treatment strategies for brain disorders.

Keywords: cannabinoid receptor; allosteric modulator; mycophenolate mofetil; GW-842,166X; MDA7; brain disorders

1. Introduction

The endocannabinoid system is comprised of two primary receptor subtypes, the cannabinoid receptor subtype 1 (CB_1) and subtype 2 (CB_2). While CB_1 is more abundantly expressed in the brain, CB_2 is expressed in the immune system and was initially thought to be a peripheral receptor [1,2]. CB_1 is a potential therapeutic target for indications including nausea [3], psychosis [4], anxiety [5], and pain [6]. Subsequent studies characterized CB_2 expression in the brain [7–10] and the CB_2 receptor has emerged as a therapeutic target for brain disorders ranging from anxiety [11] and depression [12], to addiction [13] and schizophrenia [14,15].

A number of CB_2 receptor agonists have been developed and tested in clinical trials for a variety of indications including pain and Alzheimer's disease and several compounds have been shown to be safe for human administration. GW-842,166X is a CB_2 selective agonist developed by GlaxoSmithKline [16,17] and was evaluated in Phase I trials for the indications of pain and inflammation (NCT00511524) and Phase II trials for dental pain (NCT00444769). The trials were either

© 2025 by the author(s). Distributed under a Creative Commons CC BY license.

Preprints.org (www.preprints.org) | NOT PEER-REVIEWED | Posted: 22 April 2025 doi:10.20944/preprints202504.1842.v1

withdrawn or completed with no results posted. MDA7 (NTRX-07) is a CB_2-preferring agonist developed by Naiguib et al. and NeuroTherapia [18–20]; it was progressed into Phase I trials for the indications of neuropathic pain (NCT04375436) and Alzheimer's disease (NCT06194552) and, according to press releases, this compound is progressing into Phase II studies for Alzheimer's disease.

As an alternative to direct CB_2 activation, the use of allosteric modulators may provide an improved approach by targeting neurotransmitter-dependent activity [21]. The spatial and temporal control made possible with allosteric potentiators, along with improved subtype-selectivity, suggests that efficacy may be improved with fewer adverse side effects [22,23]. The first published small molecule positive allosteric modulator (PAM) of CB_2, EC21a, has been shown to have diverse functional activity [24,25]. While reported initially as a potentiator of CB_2, it has subsequently shown inverse agonist activity in a variety of independent assays; thus, a pure PAM has yet to be identified [26,27]. To discover novel compounds with CB_2 PAM activity, we screened a collection of approximately 1000 FDA-approved drugs and identified mycophenolate mofetil as a putative PAM of the CB_2 receptor. Additional profiling, however, revealed that this compound was actually an agonist of CB_2. Mycophenolate mofetil is a widely used immunosuppressive agent [28–30]; this compound demonstrated CB_2 activity in a variety of assays, including G Protein Inwardly Rectifying Potassium (GIRK) channel-mediated thallium flux, phosphoinositide (PI) hydrolysis, cAMP inhibition, and β-arrestin recruitment. It was also selective for CB_2 versus CB_1. In contrast to the parent molecule, the active form of the drug that is responsible for immunosuppression, mycophenolic acid [28–30], was inactive at the CB_2 receptor. Radioligand binding studies indicate that mycophenolate mofetil does not interact with the binding site occupied by [^{3}H]CP55,940 in a competitive manner. During the course of our studies, we also profiled the known CB_2 agonists, GW-842,166X and MDA7. In receptor-activated GIRK assays, our studies indicated comparable agonist activity between GW-842,166X and mycophenolate mofetil but MDA7 exhibited inverse agonist activity at CB_2; however, all three compounds demonstrated agonist activity in multiple signaling pathways using cAMP inhibition and β-arrestin assays. With respect to radioligand binding, GW-842,166X exhibited comparable binding activity to mycophenolate mofetil while MDA7 displayed a different binding profile. The FDA-approved immunosuppressant mycophenolate mofetil represents a novel CB_2 agonist with unique properties compared to known CB_2 agonists. While subtle, these differences may provide insight into the mechanism of action of CB_2 modulators and prove to be significant when evaluating novel compounds as possible therapeutics for brain disorders.

2. Results

2.1. Identification of Novel Modulators of the CB_2 Receptor

To identify new compounds capable of potentiating CB_2 responses to the endogenous agonist 2-AG, we used a thallium flux assay measuring the ability of ligands to enhance 2-AG-induced responses in cells expressing rCB_2 and GIRK channels to screen a collection of FDA-approved drugs. Compounds were added to cells loaded with thallium sensitive dye and allowed to incubate for 2.3 minutes, whereupon a submaximal concentration (EC_{20}) of 2-AG was added to the cells and the signal was monitored for an additional 2.7 minutes. The ~1000 compound collection was initially screened in single point at a 10 μM concentration of compound. Test compounds that potentiated the cellular response to 2-AG by a minimum of 3 standard deviations above the average EC_{20} agonist response were selected as potential PAM hits. Sample kinetic traces of a hit from the screen, compared to EC_{20} and EC_{Max} responses to 2-AG, are shown in Figure 1. 63 putative PAMs were identified; of these, 13 were confirmed as active with concentration-dependent activity at the rCB_2 receptor.

Preprints.org (www.preprints.org) | NOT PEER-REVIEWED | Posted: 22 April 2025 doi:10.20944/preprints202504.1842.v1

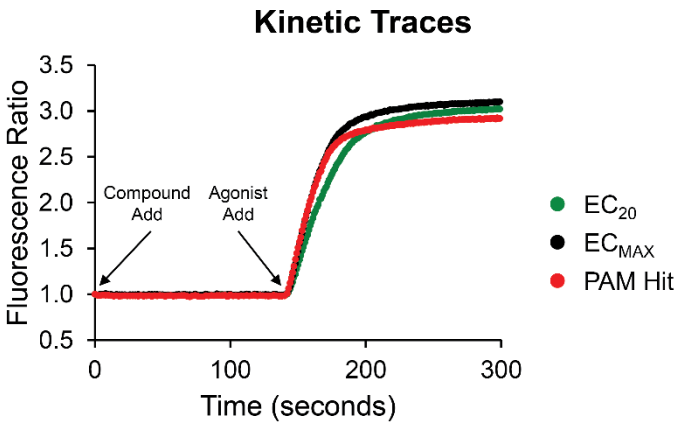

Figure 1. Sample traces from screen of FDA collection exemplify a PAM hit. Test compounds or vehicle were added at t=1 second and the fluorescence ratio was monitored. Agonist was added at t = 141 seconds**.** Fluorescence readings for each time point in a well were divided by the fluorescence reading at the initial time point to account for differences in cell number, non-uniform illumination, and dye-loading. The slope value for each kinetic trace was calculated for the time window of 145-155 seconds. The average slope was calculated for wells containing vehicle and this value was subtracted from all wells. Vehicle-subtracted slope was normalized to the relevant maximal agonist signal for each assay. Traces for a sub-maximal agonist response (EC_{20}, green) are compared to a maximal response (EC_{Max}, black) and PAM hit (red).

2.2. Mycophenolate Mofetil is a Potent and Selective Activator of rCB2

One hit in particular, mycophenolate mofetil (Figure 2A, white circles), exhibited robust potency and efficacy at rCB_2 (pEC_{50} = 6.64 ± 0.06, 228 nM; 74 ± 2 % Max) and was selected for additional studies. Mycophenolate mofetil is an immunosuppressant used to prevent organ transplant rejection and to treat autoimmune disorders such as lupus [28–30]. To determine if mycophenolate mofetil exerts its activity in the thallium flux assay through rCB_2, we tested it for activity in HEK cells expressing GIRK channels but not rCB_2. Submaximal concentrations of acetylcholine were used as the agonist, targeting the endogenous M_4 muscarinic receptor expressed in HEK/GIRK cells [31]. Mycophenolate mofetil was found to be inactive under these conditions (Figure 2A, red circles), suggesting that its activity is dependent on the presence of the rCB_2 receptor. It was also critical to determine if mycophenolate mofetil was selective for the rCB_2 versus rCB_1 receptors, as activation of rCB_1 receptors can have negative side effects including anxiety, paranoia, and psychosis [32-34]. To determine subtype selectivity, mycophenolate mofetil was tested for activity in cells co-expressing rCB_1 and GIRK channels using thallium flux. The compound did not enhance the agonist-induced response; however, mycophenolate mofetil exhibited a small inhibition of the rCB_1 response to 2-AG at high concentrations. Results are shown in Figure 2A (blue circles, pEC_{50} < 5, -5.5 ± 1.1 % Max). Mycophenolate mofetil was also tested for activity at the human CB_2 receptor and found to be active (pEC_{50} = 5.70 ± 0.11; 36 ± 4 % Max, data[32–34 not shown).

Preprints.org (www.preprints.org) | NOT PEER-REVIEWED | Posted: 22 April 2025 doi:10.20944/preprints202504.1842.v1

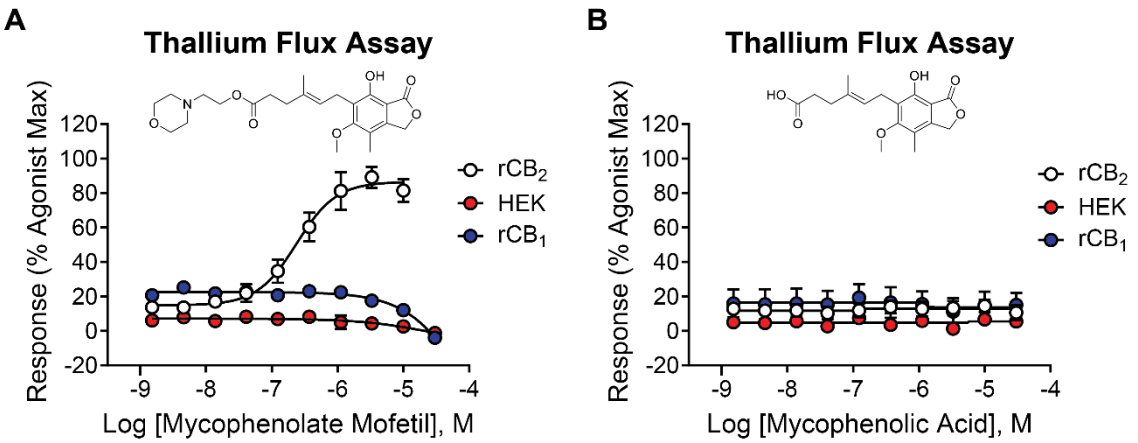

Figure 2. Mycophenolate mofetil is potent and selective for rCB_2 while mycophenolic acid is inactive at CB receptors and parental HEK/GIRK cells. Concentration-response curves in thallium flux assays for (A) mycophenolate mofetil and (B) mycophenolic acid in the presence of a sub-maximal (EC_{20}) concentration of agonist (2-AG or acetylcholine). Results are shown for rCB_2 (white), HEK/GIRK (red), and rCB_1 (blue) cells. Data represent the mean ± SEM of at least three independent experiments run in duplicate or triplicate, except for mycophenolic acid at HEK/GIRK cells which was run in two independent experiments. Data are plotted as a percentage of maximal 2-AG response for rCB_2 and rCB_1 or acetylcholine response for HEK/GIRK cells.

2.3. Mycophenolic Acid Is Inactive at CB Receptors

Mycophenolic acid is the active form of mycophenolate mofetil when used as an immunosuppressive drug or for the treatment of autoimmune disorders [35]. The morpholino ethyl ester of mycophenolic acid is a prodrug form which is rapidly metabolized to the active acid in the liver. Mycophenolic acid is a potent inhibitor of inosine-5′-monophosphate dehydrogenase [36]. To test the activity of this active metabolite, the acid was evaluated for activity at rCB_2, rCB_1, and parental HEK/GIRK cells using the thallium flux assay. It was found to be inactive when tested in each of these cell lines (Figure 2B), indicating mycophenolate mofetil, as opposed to the acid, is the active form of the molecule in rCB_2 cells.

2.4. Mycophenolate Mofetil Has Similar Activity in the Presence and Absence of 2-AG in Thallium Flux Assays

The initial high throughput screen and secondary assays were performed in the presence of a submaximal (EC_{20}) concentration of 2-AG to screen for PAMs, compounds that enhance the response of the receptor to an agonist. In the assay design used here, it is possible that compounds may have activity on their own in the absence of 2-AG and would instead be classified as agonists. To distinguish between these possibilities, mycophenolate mofetil was tested for activity in the presence and absence of 2-AG in cells expressing rCB_2/GIRK or rCB_1/GIRK using thallium flux. Increasing concentrations of mycophenolate mofetil enhanced the response of rCB_2/GIRK cells in a concentration-dependent manner with similar potency and efficacy values in the absence of 2-AG (Figure 3, red circles, pEC_{50} = 6.81 ± 0.12, 154 nM; 71 ± 5 % Max). Comparing this activity to the PAM assay performed in Figure 2A shows that the only difference in activity between the two experiments is the elevated baseline observed in the presence of agonist due to the EC_{20} response of 2-AG. These results suggest that mycophenolate mofetil acts as an agonist as opposed to a PAM in rCB_2/GIRK cells using thallium flux as a measure of activity. Mycophenolate mofetil decreased the response of rCB_1/GIRK cells both in the presence (Figure 2A, blue circles) and absence (Figure 3, black circles, pEC_{50} < 5, -15 ± 3 % Max) of 2-AG to a similar value, again differentiated only by the EC_{20} response of 2-AG. In rCB_1/GIRK cells, mycophenolate mofetil decreases the signal below baseline when added alone, although weakly, which may suggest inverse agonist activity. The decrease in signal in the

Preprints.org (www.preprints.org) | NOT PEER-REVIEWED | Posted: 22 April 2025 doi:10.20944/preprints202504.1842.v1

presence of 30 μM mycophenolate mofetil compared to baseline is significant when added alone (p=0.002) and in the presence of 2-AG (p = 0.0003).

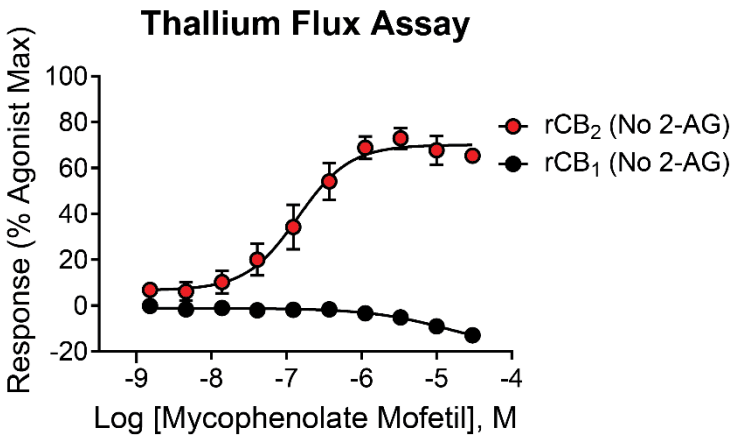

Figure 3. Mycophenolate mofetil is active at CB receptors in the absence of 2-AG. Concentration-response curves in thallium flux assays for mycophenolate mofetil in the absence of agonist. Results are shown for rCB_2 (red) and rCB_1 (black) cells. Data represent the mean ± SEM of at least three independent experiments run in duplicate or triplicate. Data are plotted as a percentage of maximal 2-AG response.

2.5. The Antagonist/Inverse Agonist AM630 Shifts the Mycophenolate Mofetil Concentration-Response Curve (CRC) to the Right Without Significantly Decreasing the Maximal Response

To further characterize the activity of mycophenolate mofetil, we investigated the effect of orthosteric antagonist/inverse agonist AM630 [37–40] on the concentration-response of rCB_2 cells to mycophenolate mofetil. If AM630 and mycophenolate mofetil bind to the same site on the receptor, increasing concentrations of AM630 would be expected to shift the CRC to the right with no decrease in maximal response, a pattern indicative of a competitive interaction. As seen in Figure 4, AM630 had little effect on the response to mycophenolate mofetil at or below a concentration of 1 μM. At 3 and 10 μM, AM630 significantly shifted the CRC to the right compared to vehicle (pEC_{50} vehicle = 6.47 ± 0.16; pEC_{50} 3 μM AM630 = 5.68 ± 0.09 (p = 0.01), pEC_{50} 10 μM AM630 = 5.64 ± 0.16 (p = 0.02). There was no significant change in maximum signal compared to vehicle with either 3 or 10 μM AM630. While these results are not conclusive on their own, they suggest mycophenolate mofetil may have a competitive relationship with AM630.

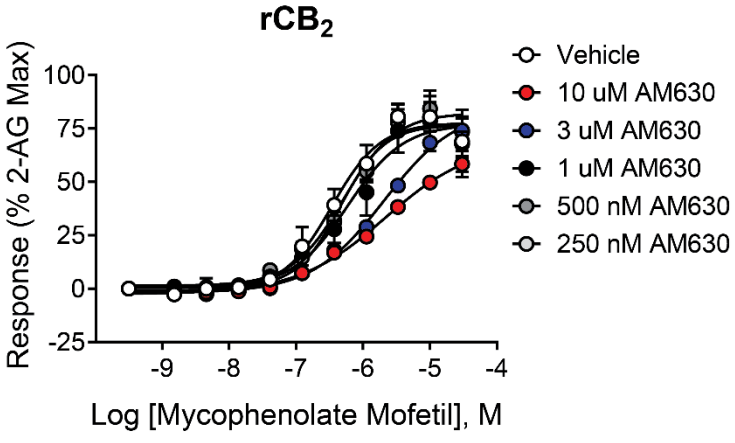

Figure 4. Increasing concentrations of AM630 shifts the CRC of mycophenolate mofetil in cells expressing rCB_2. Concentration-response curves (CRCs) in thallium flux assays for mycophenolate mofetil in the presence

Preprints.org (www.preprints.org) | NOT PEER-REVIEWED | Posted: 22 April 2025 doi:10.20944/preprints202504.1842.v1

of AM630. Data represent the mean ± SEM of at least three independent experiments run in duplicate or triplicate. Data are plotted as a percentage of maximal 2-AG response.

2.6. Mycophenolate Mofetil Is Active in Phosphoinositide Hydrolysis Assays and Demonstrates Similar Activity in the Presence and Absence of 2-AG

While mycophenolate mofetil demonstrated potent agonist activity using thallium flux assays, it is important to confirm activity employing an assay that utilizes an alternate signaling pathway as CB receptors exhibit assay-dependent pharmacology [23,26,27,41–44]. In a complementary assay, we used phosphoinositide (PI) hydrolysis in the presence of the chimeric G protein, G_{qi9}, to assess activity. As seen in Figure 5, increasing concentrations of mycophenolate mofetil significantly increased PI hydrolysis in a concentration-dependent manner. Similar results were found in the presence (white circles, pIC_{50} = 6.15 ± 0.09, 700 nM; 633 ± 122 Max IP1) and absence (red circles, pIC_{50} = 6.28± 0.11, 521 nM; 438 ± 32 Max IP1) of 2-AG. These data are consistent with results from thallium flux assays, demonstrating mycophenolate mofetil acts as a CB_2 agonist in two distinct signaling pathways.

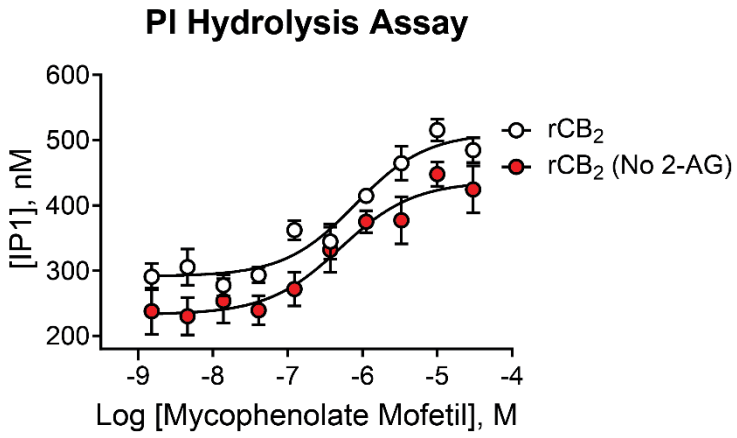

Figure 5. Mycophenolate mofetil has similar activity in presence and absence of 2-AG in PI hydrolysis. Concentration-response curves in PI hydrolysis assays for mycophenolate mofetil in the presence (white) and absence (red) of a sub-maximal (EC_{20}) concentration of agonist in cells expressing rCB_2. Data represent the mean ± SEM of three independent experiments run in duplicate or triplicate. Data are plotted as IP1 concentration in nM.

2.7. The CB_2 Receptor Agonist GW-842,166X Exhibits a Similar Functional Activity Profile Compared to Mycophenolate Mofetil

GW-842,166X is a CB_2 receptor agonist that demonstrates analgesic and anti-inflammatory activity in animal models [16,45,46] and was in clinical trials for inflammation and pain [1,47]. It is structurally distinct from mycophenolate mofetil and was selected as a comparator for these studies (see Table 1 for structure). When tested for activity in rCB_2/GIRK cells using thallium flux, GW-842,166X exhibited potent activity in the presence (white circles, pEC_{50} = 7.13 ± 0.08, 74 nM; 82 ± 4 % Max) and absence (red circles, pEC_{50} = 7.26 ± 0.05, 56 nM; 89 ± 5 % Max) of 2-AG as seen in Figure 6A. GW-842,166X was inactive at rCB_1 in both the presence (blue circles) and absence (black circles) of 2-AG. Overall, GW-842,166X exhibits a similar functional activity profile in thallium flux assays as that seen with mycophenolate mofetil.

Preprints.org (www.preprints.org) | NOT PEER-REVIEWED | Posted: 22 April 2025 doi:10.20944/preprints202504.1842.v1

Table 1. Activity of CB_2 compounds in thallium flux and binding assays.

Compound	rCB_2 GIRK		rCB_1 GIRK		HEK GIRK	rCB_2 Binding
	PAM Activity pEC_{50} ± SEM % Max ± SEM	**AGO Activity pEC_{50} ± SEM % Max ± SEM**	**PAM Activity pEC_{50} ± SEM % Max ± SEM**	**AGO Activity pEC_{50} ± SEM % Max ± SEM**	**PAM Activity pEC_{50} ± SEM % Max ± SEM**	**Binding Affinity pK_i ± SEM % Max ± SEM**
mycophenolate mofetil 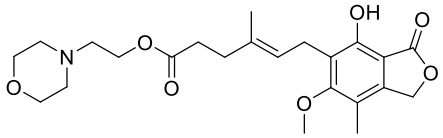	6.64 ± 0.06 74 ± 2 %	6.81 ± 0.12 71 ± 5 %	< 5.0 -5.5 ± 1.1 %	< 5.0 -15 ± 3 %	Inactive	Incomplete pEC_{50} < 5.0 20 ± 1
mycophenolic acid 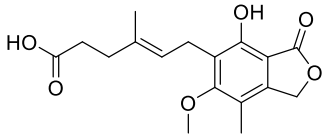	Inactive	ND	Inactive	ND	Inactive	ND
GW-842,166X 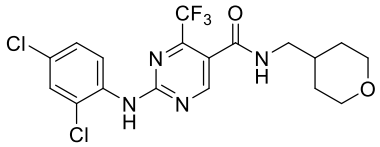	7.13 ± 0.08 82 ± 4 %	7.26 ± 0.05 89 ± 5 %	Inactive	Inactive	ND	Incomplete pEC_{50} < 5.0 22 ± 2
MDA7 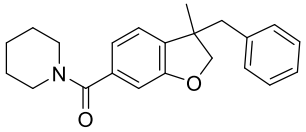	< 5.0 -65 ± 15%	< 5.0 -64 ± 13%	6.40 ± 0.02 48 ± 2	6.32 ± 0.03 50 ± 2	ND	6.60 ± 0.05 5.3 ± 1.7

*ND indicates not determined.

Preprints.org (www.preprints.org) | NOT PEER-REVIEWED | Posted: 22 April 2025 doi:10.20944/preprints202504.1842.v1

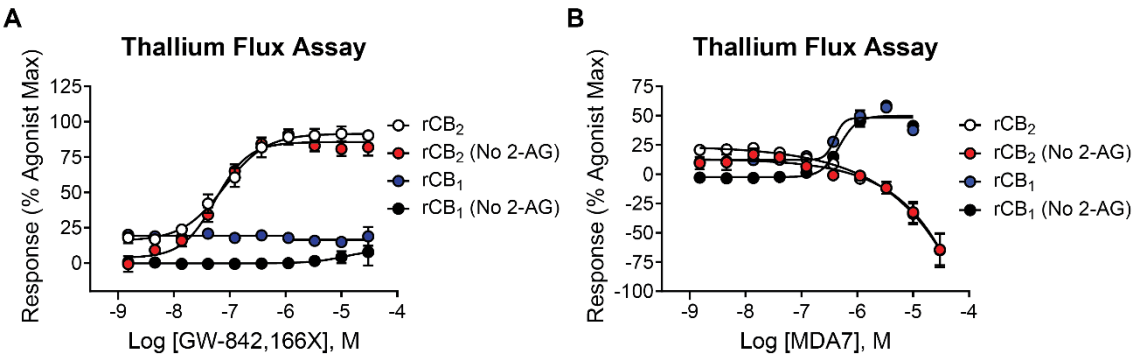

Figure 6. The CB_2 agonists GW-842,166X and MDA7 exhibit distinctions in pharmacological activity in rCB_2 thallium flux assays. Concentration-response curves in thallium flux assays are shown for GW-842,166X (A) and MDA7 (B). Results are presented for rCB_2 in the presence (white) or absence (red) of a sub-maximal (EC_{20}) concentration of agonist. Results are presented for rCB_1 in the presence (blue) or absence (black) of a sub-maximal (EC_{20}) concentration of agonist. Data represent the mean ± SEM of three independent experiments run in duplicate or triplicate. Data are plotted as a percentage of maximal 2-AG response.

2.8. In Contrast to Mycophenolate Mofetil and GW-842,166X, the CB_2 Receptor Agonist MDA7 Exhibits Inverse Agonist Activity at rCB_2 in Thallium Flux Assays.

MDA7 is a CB_2 receptor modulator structurally distinct from both mycophenolate mofetil and GW-842,166X and was described as exhibiting agonist activity at CB_2 in GTPγS assays [18–20]. Studies reported MDA7 as active in models of inflammation and neuropathic pain [20,48–50] and the compound was shown to induce neuroprotective effects in rodent models [51–53]. Currently, MDA7 is being evaluated as a novel therapeutic for the treatment of Alzheimer's disease [1,47]. To compare to the other agonists described above, we tested MDA7 for activity in both rCB_2/GIRK and rCB_1/GIRK cells using thallium flux. In contrast to both mycophenolate and GW-842,166X, MDA7 exhibited inhibitory activity in the presence (white circles, $pEC_{50} < 5$, -65 ± 15 Max) and absence (red circles, $pEC_{50} < 5$, -64 ± 13 Max) of 2-AG stimulation of rCB_2 as seen in Figure 6B. In contrast, MDA7 activated rCB_1 in the presence (blue circles, $pEC_{50} = 6.40 \pm 0.02$, 395 nM; 48 ± 2 % Max) and absence (black circles, $pEC_{50} = 6.32 \pm 0.03$, 477 nM; 50 ± 2 % Max) of 2-AG (Figure 6B). The detection of opposing CB_2 activity in assays that target differential signaling pathways is difficult to predict but is not unanticipated, as it has been observed with other CB receptor modulators [26,27,54–59].

2.9. Mycophenolate Mofetil and Other CB_2 Modulators Differentially Bind to the Site Occupied by [^{3}H]CP55,940

Results from functional assays including thallium flux and PI hydrolysis indicate that mycophenolate mofetil acts as an agonist of rCB_2 due to its ability to activate the receptor when added alone to cells expressing rCB_2; however, these assays do not provide information about the binding interaction between the receptor and mycophenolate mofetil. Agonists that bind to the receptor at the site occupied by the endogenous ligand, 2-AG in this case, are considered orthosteric agonists. It is also possible for an agonist to bind and activate a receptor via a site other than the orthosteric site; these ligands are classified as allosteric agonists. To characterize the nature of the agonist activity of mycophenolate mofetil, we tested its ability to bind to the receptor in equilibrium binding assays using membranes harvested from cells expressing rCB_2 using the radioligand [^{3}H]CP55,940 [40,60]. CP55,940 has an affinity for both CB_1 and CB_2 receptors in the low nM range and is reported to bind to the site occupied by 2-AG [61]. The CB_2 antagonist/inverse agonist AM630 fully inhibited radioligand binding with a pK_i value of 7.61 ± 0.29, results consistent with those described in the literature [40]. Increasing concentrations of mycophenolate mofetil had little effect on the equilibrium binding of [^{3}H]CP55,940 until reaching 1 μM and did not fully displace the binding when tested up to 30 μM (Figure 7, Table 1). Similar results were observed for the agonist GW-842,166X. The

Preprints.org (www.preprints.org) | NOT PEER-REVIEWED | Posted: 22 April 2025 doi:10.20944/preprints202504.1842.v1

incomplete binding and discrepancy between the functional potency and binding affinity of these ligands suggest an overlapping or alternate binding site as opposed to a competitive interaction. In contrast, the CB_2 modulator MDA7 fully inhibited radioligand binding with a pK_i value of 6.60 ± 0.05. These binding results on their own suggest that MDA7 occupies the same site as [^{3}H]CP55,940; however, the inverse agonist functional results suggest additional assays are needed to characterize the interaction.

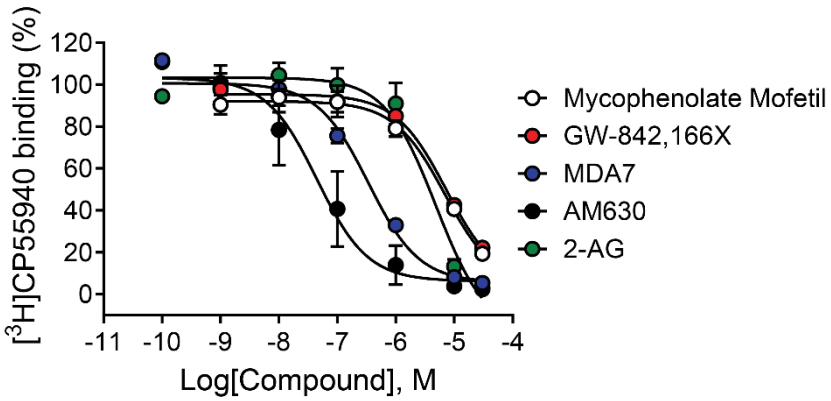

Figure 7. CB receptor ligands exhibit varying effects on [^{3}H]CP55,940 binding under equilibrium conditions. Competition binding concentration-response curves were obtained in the presence of 0.5 nM [^{3}H]CP55,940 using membranes harvested from HEK/GIRK cells expressing rCB_2. Data represent the mean ± SEM of three independent experiments run in triplicate. Data are plotted as a percentage of specific [^{3}H]CP55,940 binding. Non-specific binding was determined in the presence of 10 μM CP55,940.

2.10. Mycophenolate Mofetil, GW-842,166X, and MDA7 Behave as Agonists in cAMP and β-Arrestin Assays

Recent publications highlight the complex pharmacology of CB_2 modulators such as EC21a and the importance of profiling CB_2 modulators in assays that target different signaling pathways [26,27,43,55,59]. We have described results for thallium flux assays that measure CB receptor-mediated opening of GIRK channels and PI hydrolysis assays measuring activity via a chimeric G protein. We also evaluated the ability of mycophenolate mofetil and its comparators to modulate CB_2 through two additional pathways, cAMP inhibition and β-arrestin recruitment. When added in the presence (Figure 8A) or absence (Figure 8C) of an EC_{20} concentration of the agonist CP55,940, mycophenolate mofetil, GW-842,166X, and MDA7 all enhanced the cAMP response to CP55,940 in cells expressing human CB_2 receptors. The potency values for each (Table 2) were right-shifted compared to those observed for the thallium flux assay (Table 1). Mycophenolate mofetil also exhibited lower efficacy in cAMP assays compared to thallium flux and versus GW-842,166X and MDA7. Similarly, when tested in a β-arrestin recruitment assay in the presence (Figure 8B) or absence (Figure 8D) of an EC_{20} concentration of the agonist CP55,940, mycophenolate mofetil, GW-842,166X, and MDA7 also induced similar responses in the absence and presence of CP55,940 and potency values were generally right-shifted compared to thallium flux assays. MDA7 was notable in that its efficacy was lower than the other two ligands with and without 2-AG when β-arrestin recruitment was measured. These data confirm mycophenolate mofetil and comparator GW-842,166X demonstrate agonist activity across multiple assays and signaling pathways and also confirm the signal bias induced by MDA7.

Preprints.org (www.preprints.org) | NOT PEER-REVIEWED | Posted: 22 April 2025 doi:10.20944/preprints202504.1842.v1

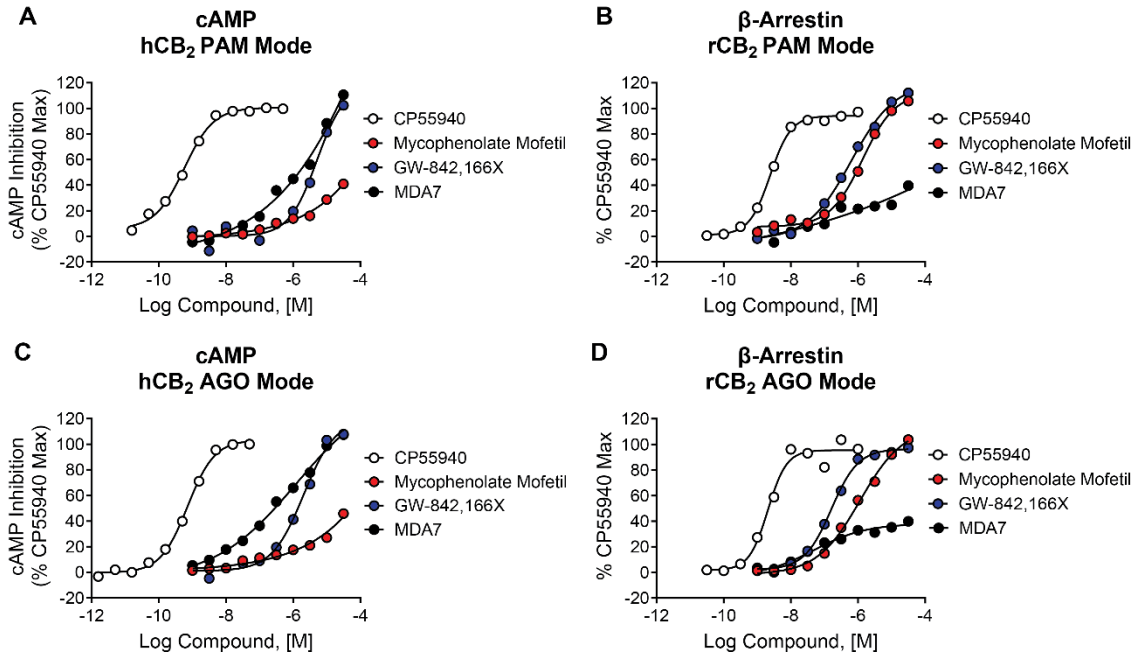

Figure 8. Differential activity of CB_2 agonists in cAMP and β-arrestin assays. Concentration-response curves in cAMP assays in the presence (A) and absence (C) of agonist are shown for CP55,940 (white), mycophenolate mofetil (red), GW-842,166X (blue) and MDA7 (black). Concentration-response curves in β-arrestin recruitment assays in the presence (B) and absence (D) of agonist are shown for CP55,940 (white), mycophenolate mofetil (red), GW-842,166X (blue) and MDA7 (black). Data represent one independent experiment run in duplicate. Data are plotted as a percentage of maximal CP55,940 response.

Table 2. Activity of CB_2 compounds in cAMP and β-arrestin assays.

Compound	hCB2 cAMP		rCB2 β-Arrestin	
	PAM Activity pEC50 % Max	AGO Activity pEC50 % Max	PAM Activity pEC50 % Max	AGO Activity pEC50 % Max
mycophenolate mofetil	< 5.0 41	< 5.0 46	5.87 113	5.94 114
GW-842,166X	5.29 119	5.69 120	6.20 120	6.79 97
MDA7	< 5.0 111	< 5.0 108	< 5.0 40	7.32 38

3. Discussion

The endocannabinoid system, composed of CB_1 and CB_2 receptors, has been extensively studied as a possible therapeutic target for various neurological and inflammatory disorders. CB_1 is widely expressed across brain regions, while CB_2 is primarily expressed in the immune system and microglia [1,2]. Recent studies have shown CB_2 expression in hippocampal, striatal, and dopaminergic neurons, suggesting the potential for CB_2 modulation for the treatment of disorders including pain, addiction, and schizophrenia [1,13–15,47,62,63]. Reduced CB_2 receptor expression and activity is correlated with an increased risk of developing schizophrenia [64–67]. We have shown that the antipsychotic effects of muscarinic M_4 receptor or metabotropic glutamate receptor 1 ($mGlu_1$) PAMs in rodent behavioral

Preprints.org (www.preprints.org) | NOT PEER-REVIEWED | Posted: 22 April 2025 doi:10.20944/preprints202504.1842.v1

models are dependent on CB_2 activation, which occurs via retrograde signaling of 2-AG [14,15]. For these reasons, it is possible that CB_2 activation or potentiation may represent a novel strategy for treatment. The use of a PAM as opposed to an agonist may provide advantages, as a PAM would be predicted to produce lower levels of receptor desensitization and greater receptor specificity [22,23]. We recently profiled the first published small molecule PAM, EC21a, showing that this ligand exhibits complex pharmacology [26]. To discover novel CB_2 PAMs with improved properties compared to EC21a, we conducted a screen of FDA-approved drugs, resulting in the discovery of immunosuppressant mycophenolate mofetil as a selective activator of CB_2.

The initial design of the assay was intended to screen for PAMs, but subsequent assays determined mycophenolate mofetil was active in the absence of agonist. Other CB_2 agonists have been or are currently being studied in preclinical and clinical trials including GW-842,166X for pain [16,45,46] and MDA7 for pain [49,50,68] and Alzheimer's disease [51,52], but to date no CB_2 agonist drugs are approved for clinical use. As shown here, both mycophenolate mofetil and GW-842,166X present clear profiles as selective agonists of CB_2 in multiple assays assessing various signaling pathways including thallium flux, cAMP, and β-arrestin assays. MDA7 instead exhibits a mixed profile. In cAMP and β-arrestin assays, it acts as an agonist of the CB_2 receptor; however, in thallium flux assays MDA7 demonstrates inverse agonist activity, clearly blocking the basal signal well below baseline levels. It is also not selective for CB_2 in thallium flux assays as it also significantly activates the CB_1 receptor. It is possible that this mixed activity profile may present challenges when assessing for potential utility as a treatment for brain disorders.

The binding data generated with [^{3}H]CP55,940 indicate multiple binding modes/sites are present within the CB_2 receptor. 2-AG is reported to share the same orthosteric binding site as CP55,940 [61] and we confirmed that 2-AG fully displaced radioligand binding ($pK_i = 5.46 \pm 0.05$). Additionally, the inverse agonist AM630 fully inhibited the equilibrium binding of the radioligand with a K_i value consistent with that reported in the literature ($pK_i = 7.61 \pm 0.29$) [40]. Mycophenolate mofetil was only able to inhibit radioligand binding to a level equal to 20% of [^{3}H]CP55,940 total binding at 30 μM. This level of binding indicates a potential interaction with the binding site occupied by the radioligand, but the disconnect between the binding data and the functional potency generated in the same cell line (rCB_2/GIRK) using thallium flux suggests the binding of mycophenolate mofetil is not completely competitive with [^{3}H]CP55,940. It is possible the two ligands occupy the same site but have different binding contacts or that the ligands share an overlapping portion of the site. It will be important to fully characterize the binding mode of mycophenolate mofetil using mutagenesis and additional molecular pharmacology studies to more fully understand the binding and functional relationship and how it relates to future drug development. This is also the case for GW-842,166X, which exhibited a similar binding profile to that of mycophenolate mofetil with incomplete binding reaching 20% of [^{3}H]CP55,940 total binding. The potency value of this compound in thallium flux assays ($pEC_{50} = 7.13$) revealed a left-shifted pEC_{50} compared to the K_i. MDA7, on the other hand, presents a different profile and fully inhibited the equilibrium binding of [^{3}H]CP55,940 ($pK_i = 6.60 \pm 0.05$). In the rCB_2/GIRK cell line measuring thallium flux, MDA7 displayed weak inverse agonist activity with a potency value significantly right-shifted in comparison ($pEC_{50} < 5.0$). The complete inhibition in the binding assay suggests a competitive interaction with the [^{3}H]CP55,940 binding site, but the weak blockade in the functional assay indicates a disconnect between the binding affinity and the functional potency in the thallium flux assay.

In this study, we discovered that mycophenolate mofetil is a selective agonist of CB_2 through screening of an FDA-approved library of drugs. Its agonist activity was confirmed in multiple assays assessing activity through different signaling pathways, including thallium flux, PI hydrolysis, cAMP inhibition, and β-arrestin recruitment. The activity profiles of the CB_2 clinical candidates GW-842,166X and MDA7 were assessed and found to be similar to mycophenolate mofetil in the case of GW-842,166X but divergent for MDA7. These findings suggest that modulators of CB_2 have subtle pharmacological complexities and understanding these differences may provide insight into

Preprints.org (www.preprints.org) | NOT PEER-REVIEWED | Posted: 22 April 2025 doi:10.20944/preprints202504.1842.v1

developing better treatments for brain disorders such as schizophrenia, pain, and Alzheimer's disease.

4. Materials and Methods

4.1. Chemicals

2-Arachidonoylglycerol (2-AG) and 6-iodo-2-methyl-1-[2-(4-morpholinyl)ethyl]-1H-indol-3-yl](4-methoxyphenyl)methanone (AM630) were purchased from Cayman Chemical (Ann Arbor, MI). 2-[(1*R*,2*R*,5*R*)-5-hydroxy-2-(3-hydroxypropyl)cyclohexyl]-5-(2-methyloctan-2-yl)phenol (CP55,940) was purchased from Tocris Bioscience (Minneapolis, MN). [^{3}H]-CP55,940 was obtained from Perkin Elmer (Boston, MA). 2-(2,4-dichloroanilino)-N-(oxan-4-ylmethyl)-4-(trifluoromethyl)pyrimidine-5-carboxamide (GW-842,166X) and 1-[(3-benzyl-3-methyl-2,3-dihydro-1-benzofuran-6-yl)carbonyl]piperidine (MDA7/NTRX-07) were synthesized by the Warren Center for Neuroscience Drug Discovery, Vanderbilt University, Nashville, USA as previously described [16,18–20].

4.2. Cell Culture

Human Embryonic Kidney (HEK) 293 cells stably expressing rCB_2 and the G protein G_{qi9} were maintained in Dulbecco's modified Eagle media (DMEM) containing 10% FBS, 1x antibiotic/antimycotic, 20 mM HEPES, 1 mM sodium pyruvate, 2 mM L-glutamine, 1x non-essential amino acids, 700 µg/mL G418 sulfate, and 0.6 µg/mL puromycin. HEK cells stably expressing rCB_2 or rCB_1 and the G protein inwardly rectifying potassium channel (GIRK) were maintained in DMEM/F12 containing 10% FBS, 1x antibiotic/antimycotic, 20 mM HEPES, 1 mM sodium pyruvate, 2 mM L-glutamine, 1x non-essential amino acids, 700 µg/mL G418 sulfate, and 0.6 µg/mL puromycin. Cells were monitored by periodic PCR detection using the LookOut Mycoplasma PCR Detection Kit (Sigma-Aldrich, St Louis, MO) to eliminate potential mycoplasma infection. Reagents were obtained from Invitrogen (Waltham, MA) unless otherwise noted.

4.3. Thallium Flux Assay

Thallium flux assays were performed as previously described in Niswender et al., 2008 [31]. HEK/GIRK cells stably expressing rCB_1 or rCB_2 (15,000 cells/20 µL/well) were seeded in 384-well, poly-D-lysine coated assay plates (Corning BioCoat®) (Corning Inc., Corning, NY) and incubated overnight at 37 °C in the presence of 5% CO_2. The next day, medium was removed and replaced with 20 µL of 1.2 µM thallium-sensitive dye Thallos-AM (ION biosciences, San Marcos, TX), prepared as a DMSO stock solution mixed in a 1:1 ratio with 10% (w/v) pluronic acid F-127, and diluted in assay buffer (Hank's balanced salt solution, 20 mM HEPES, pH 7.4). Following 1 hour at room temperature, dye solution was removed and replaced with 20 µL assay buffer. For screening of the FDA-Approved Drug Collection, 10 mM DMSO stocks of library compounds were transferred to daughter plates using an Echo acoustic plate reformatter (Labcyte, Sunnyvale, CA) and diluted in assay buffer to a 2x final concentration. For concentration-response curve experiments, compounds were serially diluted 1:3 into 10-point concentration response curves in DMSO, transferred to daughter plates using the Echo or Bravo Automated Liquid Handling Platform (Agilent Technologies, Santa Clara, CA), and diluted in assay buffer to a 2x final concentration. Thallium flux was measured using the Hamamatsu FDSS/µCELL Kinetic Plate Imager (Bridgewater, NJ). After establishment of a fluorescence baseline (excitation, 480 ± 20 nm; emission, 540 ± 30 nm), 20 µL (2x) of test compound was added to the cells at 1 second and the response was measured. 140 seconds later, 10 µL (5x) of an EC_{20} concentration of agonist (PAM mode) or vehicle (AGO mode) in thallium stimulus buffer (125 mM $NaHCO_3$, 1.8 mM $CaSO_4$, 1 mM $MgSO_4$, 5 mM glucose, 12 mM Tl_2SO_4, 10 mM HEPES, 0.5% BSA, pH 7.4) was added to the cells, and the response of the cells was measured for an additional 159 seconds (data were acquired for 300 seconds total at 0.5 Hz for 140 seconds and 1 Hz for 160 seconds). Raw kinetic data were analyzed in a multi-step process. 1) Fluorescence readings for each time point in a well were

Preprints.org (www.preprints.org) | NOT PEER-REVIEWED | Posted: 22 April 2025 doi:10.20944/preprints202504.1842.v1

divided by the fluorescence reading at the initial time point to account for differences in cell number, non-uniform illumination, and dye-loading. 2) The slope value for each kinetic trace was calculated for the time window of 145-155 seconds, a window occurring directly after the second addition. 3) The average slope was calculated for wells containing vehicle and this value was subtracted from all wells. 4) Vehicle-subtracted slope was normalized to the relevant maximal agonist signal for each assay. For concentration response curves, normalized data were fit to a four-parameter logistic equation using GraphPad Prism (La Jolla, CA) or the Dotmatics software platform (Dotmatics, Bishop's Stortford, UK).

$$y = bottom + \frac{top - bottom}{1 + 10^{(LogEC50 - A)Hillslope}}$$

where A is the molar concentration of the compound; *bottom* and *top* denote the lower and upper plateaus of the concentration-response curve; Hillslope is the Hill coefficient that describes the steepness of the curve; and EC_{50} is the molar concentration of compound required to generate a response halfway between the *top* and *bottom*. Data shown represent the mean ± standard error of the pEC_{50} or maximal response. Experiments were performed in duplicate or triplicate and repeated a minimum of three separate times.

4.4. PI Hydrolysis Assay

One day prior to experimentation, selected HEK/G_{qi9} monoclonal cells stably expressing rat CB_2 were plated onto poly-D-lysine coated clear-bottom 384-well plates (15,000 cells per well) in DMEM supplemented with 10% FBS and 20 mM HEPES. Ten minutes prior to the assay, cell culture medium was replaced with 20 µL 37 °C Hank's balanced salt solution (HBSS, with Ca^{2+}, Mg^{2+}, glucose). IP_1 stimulation was then initiated by adding 5 µL of 5x agonist dissolved in HBSS plus 40 mM Li^+, and cells were incubated for an additional hour before aspiration and addition of Lysis Buffer. IP_1 levels were determined using the Cisbio HTRF IP-ONE assay kit per the manufacturer's instructions, and fluorescence was measured using an Envision plate reader (PerkinElmer, Waltham, MA). Data were acquired as HTRF ratio (665/620) and expressed as nanomolar levels of IP_1.

4.5. Radioligand Binding Assays

Membranes were made from HEK/GIRK cells stably expressing rat CB_2. Radioligand competition binding assays were performed as previously described with minor modifications. In brief, compounds were serially diluted into assay buffer with 0.1% bovine serum albumin (BSA) and added to each well of a 96-well plate, along with 20 µg/well cell membrane and approximately 500 pM [^{3}H]-CP55,940 (specific activity = 104 Ci/mmol, PerkinElmer, Waltham, MA). Following a 3-hour incubation period on shaker at room temperature, the membrane-bound ligand was separated from free ligand by filtration through glass fiber 96-well filter plates (Unifilter-96, GF/B; PerkinElmer, Waltham, MA). Forty microliters of scintillation fluid were added to each well, and the membrane-bound radioactivity was determined by scintillation counting (Microbeta2; Revvity, Waltham, MA). Nonspecific binding was determined using 10 µM of cold CP55,940.

4.6. cAMP Assays

Assays were performed by Eurofins Discovery (Freemont, CA). cAMP Hunter cell lines were expanded from freezer stocks according to standard procedures. Cells were seeded in a total volume of 20 µL into white walled, 384-well microplates and incubated at 37 °C for the appropriate time prior to testing. cAMP modulation was determined using the DiscoverX HitHunter cAMP XS+ assay. For agonist determination, cells were incubated with sample in the presence of EC_{80} forskolin to induce response. Media was aspirated from cells and replaced with 10 µL HBSS/10mM HEPES. Intermediate dilution of sample stocks was performed to generate 4X sample in assay buffer and 5 µL of 4X sample was added to cells. 5 µL of 4X EC_{80} forskolin diluted in HBSS/HEPES was added and incubated at 37 °C for 30 minutes. Final assay vehicle concentration was 1%. For allosteric determination, cells were pre-incubated with sample followed by agonist induction at the EC_{20} concentration. Media was

Preprints.org (www.preprints.org) | NOT PEER-REVIEWED | Posted: 22 April 2025 doi:10.20944/preprints202504.1842.v1

aspirated from cells and replaced with 10 µL HBSS/10mM HEPES. Intermediate dilution of sample stocks was performed to generate 4X sample in assay buffer. 5 µL of 4X compound was added to the cells and incubated at room temperature or 37 °C for 5 minutes. 5 µL of 4X EC_{20} agonist was added to the cells and incubated at 37 °C for 30 minutes. EC_{80} forskolin was included.

After appropriate compound incubation, assay signal was generated through incubation with 5µL cAMP XS+ Ab reagent followed by 20 µL cAMP XS+ ED/CL lysis cocktail for one hour at room temperature. 20 µL cAMP XS+ EA reagent for two hours at room temperature. Microplates were read following signal generation with a PerkinElmer EnvisionTM instrument for chemiluminescent signal detection.

Compound activity was analyzed using CBIS data analysis suite (ChemInnovation, CA). For agonist mode assays, percentage activity is calculated using the following formula: % Activity = 100% x (1 - (mean RLU of test sample - mean RLU of MAX control) / (mean RLU of vehicle control - mean RLU of MAX control)).

For Gi positive allosteric mode assays, percentage modulation was calculated using the following formula: % Modulation =100% x (1-(mean RLU of test sample - mean RLU of MAX control) / (mean RLU of EC_{20} control - mean RLU of MAX control)).

4.7.β-. Arrestin Assays

Assays were performed by Eurofins Discovery (Freemont, CA). PathHunter cell lines were expanded from freezer stocks according to standard procedures. Cells were seeded in a total volume of 20 µL into white walled, 384-well microplates and incubated at 37 °C for the appropriate time prior to testing. For agonist determination, cells were incubated with sample to induce response. Intermediate dilution of sample stocks was performed to generate 5X sample in assay buffer. 5 µL of 5X sample was added to cells and incubated at 37 °C or room temperature for at least 120 minutes. Final assay vehicle concentration was 1%. For allosteric modulator determination, cells were pre-incubated with sample followed by agonist challenge at the EC_{20}. Intermediate dilution of sample stocks was performed to generate 5X sample in assay buffer. 5 µL of 5X sample was added to cells and incubated at 37 °C or room temperature for 15 minutes. Vehicle concentration was 1%. 5 µL of 6X EC_{20} agonist in assay buffer was added to the cells and incubated at 37 °C or room temperature for at least 120 minutes.

Assay signal was generated through a single addition of 15 µL (50% v/v) of PathHunter Detection reagent cocktail, followed by a one-hour incubation at room temperature. Microplates were read following signal generation with a PerkinElmer EnvisionTM instrument for chemiluminescent signal detection.

Compound activity was analyzed using CBIS data analysis suite (ChemInnovation, CA). For agonist mode assays, percentage activity was calculated using the following formula: % Activity = 100% x (mean RLU of test sample — mean RLU of vehicle control) / (mean MAX control ligand — mean RLU of vehicle control).

For positive allosteric mode assays, percentage modulation was calculated using the following formula: % Modulation = 100% x ((mean RLU of test sample — mean RLU of EC_{20} control) / (mean RLU of MAX control ligand — mean RLU of EC_{20} control)).

Author Contributions: Conceptualization, C.M.N.; methodology, A.L.R., A.Q., and C.M.N; formal analysis, A.L.R., A.Q., and C.M.N; investigation, A.Q., A.H., H.E.K., M.Q., (pharmacology) A.M.B., L.B., and D. W. (chemistry); resources, C.M.N. and C.W.L.; writing—original draft preparation, A.L.R.; writing—review and editing, A.L.R., C.M.N., A.Q., A.H., H.E.K., M.Q., C.W.L., A.M.B., L.B., and D. W. All authors have read and agreed to the published version of the manuscript.

Funding: This research was funded by National Institutes of Health under Grant Numbers MH119673 and MH062464, research funds from the Warren Center for Neuroscience Drug Discovery, and a generous gift from the William K. Warren Foundation.

Preprints.org (www.preprints.org) | NOT PEER-REVIEWED | Posted: 22 April 2025 doi:10.20944/preprints202504.1842.v1

Institutional Review Board Statement: Not applicable.

Data Availability Statement: The authors declare that all processed data supporting the findings of this study are available within the paper. Raw data are available on request from the corresponding author.

Acknowledgments: We thank the William K. Warren Foundation for their funding toward the Warren Center for Neuroscience Drug Discovery.

Conflicts of Interest: The authors declare no conflicts of interest.

Abbreviations

The following abbreviations are used in this manuscript:

2-AG	2-Arachidonylglycerol
AM630	6-Iodo-2-methyl-1-[2-(4-morpholinyl)ethyl]-1*H*-indol-3-yl](4-methoxyphenyl)methanone
cAMP	cyclic adenosine monophosphate
BSA	bovine serum albumin
CB_1	cannabinoid receptor subtype 1
CB_2	cannabinoid receptor subtype 2
CP55,940	2-[(1*R*,2*R*,5*R*)-5-hydroxy-2-(3-hydroxypropyl)cyclohexyl]-5-(2-methyloctan-2-yl)phenol
CRC	concentration response curve
DMEM	Dulbecco's Modified Eagle Media
DMSO	dimethyl sulfoxide
EC21a	*N*-(5-bromo-1-(4-fluorobenzyl)-4-methyl-2-oxo-1,2-dihydropyridin-3-yl)cycloheptanecarboxamide
F12	Ham's F-12 Nutrient Mixture
FBS	fetal bovine serum
FDA	Food and Drug Administration
GPCR	G protein-coupled receptor
GIRK	G protein-regulated inwardly rectifying potassium channel
GW-842,166X	2-(2,4-dichloroanilino)-N-(oxan-4-ylmethyl)-4-(trifluoromethyl)pyrimidine-5-carboxamide
HBSS	Hank's balanced salt solution
HEK	human embryonic kidney
HEPES	4-(2-hydroxyethyl)piperazine-1-ethanesulfonic acid
IP_1	inositol monophosphate
MDA7	1-[(3-benzyl-3-methyl-2,3-dihydro-1-benzofuran-6-yl)carbonyl]piperidine
$mGlu_1$	metabotropic glutamate receptor subtype 1
M_4	muscarinic acetylcholine receptor subtype 4
PAM	positive allosteric modulator
PI	phosphoinositide
SEM	standard error of the mean

References

1. García-Gutiérrez, M.S.; Torregrosa, A.B.; Navarrete, F.; Navarro, D.; Manzanares, J. A comprehensive review of the multifaceted role of cannabinoid receptor type 2 in neurodegenerative and neuropsychiatric disorders. *Pharmacol Res* **2025**, *213*, 107657, doi:10.1016/j.phrs.2025.107657.
2. Howlett, A.C.; Barth, F.; Bonner, T.I.; Cabral, G.; Casellas, P.; Devane, W.A.; Felder, C.C.; Herkenham, M.; Mackie, K.; Martin, B.R.; et al. International Union of Pharmacology. XXVII. Classification of cannabinoid receptors. *Pharmacol Rev* **2002**, *54*, 161-202, doi:10.1124/pr.54.2.161.
3. Elgohary, R.; Salama, A.; Omara, E.A. Protective Effects of Cannabis sativa on chemotherapy-induced nausea in a rat: Involvement of CB1 receptors. *Fundam Clin Pharmacol* **2023**, *37*, 137-146, doi:10.1111/fcp.12821.

Preprints.org (www.preprints.org) | NOT PEER-REVIEWED | Posted: 22 April 2025 doi:10.20944/preprints202504.1842.v1

4. Hill, M.N.; Haney, M.; Hillard, C.J.; Karhson, D.S.; Vecchiarelli, H.A. The endocannabinoid system as a putative target for the development of novel drugs for the treatment of psychiatric illnesses. *Psychol Med* **2023**, *53*, 7006-7024, doi:10.1017/S0033291723002465.
5. Haller, J.; Varga, B.; Ledent, C.; Freund, T.F. CB1 cannabinoid receptors mediate anxiolytic effects: convergent genetic and pharmacological evidence with CB1-specific agents. *Behav Pharmacol* **2004**, *15*, 299-304, doi:10.1097/01.fbp.0000135704.56422.40.
6. Quintero, J.M.; Diaz, L.E.; Galve-Roperh, I.; Bustos, R.H.; Leon, M.X.; Beltran, S.; Dodd, S. The endocannabinoid system as a therapeutic target in neuropathic pain: a review. *Expert Opin Ther Targets* **2024**, *28*, 739-755, doi:10.1080/14728222.2024.2407824.
7. Van Sickle, M.D.; Duncan, M.; Kingsley, P.J.; Mouihate, A.; Urbani, P.; Mackie, K.; Stella, N.; Makriyannis, A.; Piomelli, D.; Davison, J.S.; et al. Identification and functional characterization of brainstem cannabinoid CB2 receptors. *Science* **2005**, *310*, 329-332, doi:10.1126/science.1115740.
8. Gong, J.P.; Onaivi, E.S.; Ishiguro, H.; Liu, Q.R.; Tagliaferro, P.A.; Brusco, A.; Uhl, G.R. Cannabinoid CB2 receptors: immunohistochemical localization in rat brain. *Brain Res* **2006**, *1071*, 10-23, doi:10.1016/j.brainres.2005.11.035.
9. Onaivi, E.S.; Ishiguro, H.; Gong, J.P.; Patel, S.; Perchuk, A.; Meozzi, P.A.; Myers, L.; Mora, Z.; Tagliaferro, P.; Gardner, E.; et al. Discovery of the presence and functional expression of cannabinoid CB2 receptors in brain. *Ann N Y Acad Sci* **2006**, *1074*, 514-536, doi:10.1196/annals.1369.052.
10. García-Gutiérrez, M.S.; Pérez-Ortiz, J.M.; Gutiérrez-Adán, A.; Manzanares, J. Depression-resistant endophenotype in mice overexpressing cannabinoid CB(2) receptors. *Br J Pharmacol* **2010**, *160*, 1773-1784, doi:10.1111/j.1476-5381.2010.00819.x.
11. García-Gutiérrez, M.S.; Manzanares, J. Overexpression of CB2 cannabinoid receptors decreased vulnerability to anxiety and impaired anxiolytic action of alprazolam in mice. *J Psychopharmacol* **2011**, *25*, 111-120, doi:10.1177/0269881110379507.
12. Onaivi, E.S.; Ishiguro, H.; Sejal, P.; Meozzi, P.A.; Myers, L.; Tagliaferro, P.; Hope, B.; Leonard, C.M.; Uhl, G.R.; Brusco, A.; et al. Methods to study the behavioral effects and expression of CB2 cannabinoid receptor and its gene transcripts in the chronic mild stress model of depression. *Methods Mol Med* **2006**, *123*, 291-298, doi:10.1385/1-59259-999-0:291.
13. Ishiguro, H.; Iwasaki, S.; Teasenfitz, L.; Higuchi, S.; Horiuchi, Y.; Saito, T.; Arinami, T.; Onaivi, E.S. Involvement of cannabinoid CB2 receptor in alcohol preference in mice and alcoholism in humans. *Pharmacogenomics J* **2007**, *7*, 380-385, doi:10.1038/sj.tpj.6500431.
14. Foster, D.J.; Wilson, J.M.; Remke, D.H.; Mahmood, M.S.; Uddin, M.J.; Wess, J.; Patel, S.; Marnett, L.J.; Niswender, C.M.; Jones, C.K.; et al. Antipsychotic-like Effects of M4 Positive Allosteric Modulators Are Mediated by CB2 Receptor-Dependent Inhibition of Dopamine Release. *Neuron* **2016**, *91*, 1244-1252, doi:10.1016/j.neuron.2016.08.017.
15. Yohn, S.E.; Foster, D.J.; Covey, D.P.; Moehle, M.S.; Galbraith, J.; Garcia-Barrantes, P.M.; Cho, H.P.; Bubser, M.; Blobaum, A.L.; Joffe, M.E.; et al. Activation of the mGlu$_1$ metabotropic glutamate receptor has antipsychotic-like effects and is required for efficacy of M4 muscarinic receptor allosteric modulators. *Mol Psychiatry* **2020**, *25*, 2786-2799, doi:10.1038/s41380-018-0206-2.
16. Giblin, G.M.; O'Shaughnessy, C.T.; Naylor, A.; Mitchell, W.L.; Eatherton, A.J.; Slingsby, B.P.; Rawlings, D.A.; Goldsmith, P.; Brown, A.J.; Haslam, C.P.; et al. Discovery of 2-[(2,4-dichlorophenyl)amino]-N-[(tetrahydro- 2H-pyran-4-yl)methyl]-4-(trifluoromethyl)- 5-pyrimidinecarboxamide, a selective CB2 receptor agonist for the treatment of inflammatory pain. *J Med Chem* **2007**, *50*, 2597-2600, doi:10.1021/jm061195+.
17. Ostenfeld, T.; Price, J.; Albanese, M.; Bullman, J.; Guillard, F.; Meyer, I.; Leeson, R.; Costantin, C.; Ziviani, L.; Nocini, P.F.; et al. A randomized, controlled study to investigate the analgesic efficacy of single doses of the cannabinoid receptor-2 agonist GW842166, ibuprofen or placebo in patients with acute pain following third molar tooth extraction. *Clin J Pain* **2011**, *27*, 668-676, doi:10.1097/AJP.0b013e318219799a.
18. Attala, M.N.; Brown, D.L. Neuroprotective CB2 Receptor Agonists. WO 2014/011949 A2, January 16, 2014.
19. Attala, M.N.; Diaz, P. Heterocycle Modulators of Cannabinoid Receptors. US 9,339,486 B2, May 17, 2016.

Preprints.org (www.preprints.org) | NOT PEER-REVIEWED | Posted: 22 April 2025 doi:10.20944/preprints202504.1842.v1

20. Naguib, M.; Diaz, P.; Xu, J.J.; Astruc-Diaz, F.; Craig, S.; Vivas-Mejia, P.; Brown, D.L. MDA7: a novel selective agonist for CB2 receptors that prevents allodynia in rat neuropathic pain models. *Br J Pharmacol* **2008**, *155*, 1104-1116, doi:10.1038/bjp.2008.340.
21. Wootten, D.; Christopoulos, A.; Sexton, P.M. Emerging paradigms in GPCR allostery: implications for drug discovery. *Nat Rev Drug Discov* **2013**, *12*, 630-644, doi:10.1038/nrd4052.
22. Lindsley, C.W.; Emmitte, K.A.; Hopkins, C.R.; Bridges, T.M.; Gregory, K.J.; Niswender, C.M.; Conn, P.J. Practical Strategies and Concepts in GPCR Allosteric Modulator Discovery: Recent Advances with Metabotropic Glutamate Receptors. *Chem Rev* **2016**, *116*, 6707-6741, doi:10.1021/acs.chemrev.5b00656.
23. Gado, F.; Meini, S.; Bertini, S.; Digiacomo, M.; Macchia, M.; Manera, C. Allosteric modulators targeting cannabinoid cb1 and cb2 receptors: implications for drug discovery. *Future Med Chem* **2019**, *11*, 2019-2037, doi:10.4155/fmc-2019-0005.
24. Gado, F.; Di Cesare Mannelli, L.; Lucarini, E.; Bertini, S.; Cappelli, E.; Digiacomo, M.; Stevenson, L.A.; Macchia, M.; Tuccinardi, T.; Ghelardini, C.; et al. Identification of the First Synthetic Allosteric Modulator of the CB_2 Receptors and Evidence of Its Efficacy for Neuropathic Pain Relief. *J Med Chem* **2019**, *62*, 276-287, doi:10.1021/acs.jmedchem.8b00368.
25. Shapiro, L.; Gado, F.; Manera, C.; Escayg, A. Allosteric modulation of the cannabinoid 2 receptor confers seizure resistance in mice. *Neuropharmacology* **2021**, *188*, 108448, doi:10.1016/j.neuropharm.2021.108448.
26. Qi, A.; Han, X.; Quitalig, M.; Wu, J.; Christov, P.P.; Jeon, K.; Jana, S.; Kim, K.; Engers, D.W.; Lindsley, C.W.; et al. The cannabinoid CB_2 receptor positive allosteric modulator EC21a exhibits complicated pharmacology in vitro. *J Recept Signal Transduct Res* **2024**, *44*, 151-159, doi:10.1080/10799893.2024.2431986.
27. Farooq, Z.; Delre, P.; Iliadis, S.; Mangiatordi, G.F.; Contino, M.; Howell, L.A.; McCormick, P.J. Identification of a Cannabinoid Receptor 2 Allosteric Site Using Computational Modeling and Pharmacological Analysis. *ACS Pharmacology & Translational Science* **2025**, *8*, 423-434, doi:10.1021/acsptsci.4c00547.
28. Allison, A.C.; Eugui, E.M. Immunosuppressive and other anti-rheumatic activities of mycophenolate mofetil. *Agents Actions Suppl* **1993**, *44*, 165-188.
29. Eugui, E.M.; Allison, A.C. Immunosuppressive activity of mycophenolate mofetil. *Ann N Y Acad Sci* **1993**, *685*, 309-329, doi:10.1111/j.1749-6632.1993.tb35881.x.
30. Ritter, M.L.; Pirofski, L. Mycophenolate mofetil: effects on cellular immune subsets, infectious complications, and antimicrobial activity. *Transpl Infect Dis* **2009**, *11*, 290-297, doi:10.1111/j.1399-3062.2009.00407.x.
31. Niswender, C.M.; Johnson, K.A.; Luo, Q.; Ayala, J.E.; Kim, C.; Conn, P.J.; Weaver, C.D. A novel assay of Gi/o-linked G protein-coupled receptor coupling to potassium channels provides new insights into the pharmacology of the group III metabotropic glutamate receptors. *Mol Pharmacol* **2008**, *73*, 1213-1224, doi:10.1124/mol.107.041053.
32. Martin, R.S.; Secchi, R.L.; Sung, E.; Lemaire, M.; Bonhaus, D.W.; Hedley, L.R.; Lowe, D.A. Effects of cannabinoid receptor ligands on psychosis-relevant behavior models in the rat. *Psychopharmacology (Berl)* **2003**, *165*, 128-135, doi:10.1007/s00213-002-1240-x.
33. Gobira, P.H.; LaMar, J.; Marques, J.; Sartim, A.; Silveira, K.; Santos, L.; Wegener, G.; Guimaraes, F.S.; Mackie, K.; Lu, H.C.; et al. CB1 Receptor Silencing Attenuates Ketamine-Induced Hyperlocomotion Without Compromising Its Antidepressant-Like Effects. *Cannabis Cannabinoid Res* **2023**, *8*, 768-778, doi:10.1089/can.2022.0072.
34. Leo, L.M.; Abood, M.E. CB1 Cannabinoid Receptor Signaling and Biased Signaling. *Molecules* **2021**, *26*, doi:10.3390/molecules26175413.
35. Allison, A.C.; Eugui, E.M. Immunosuppressive and other effects of mycophenolic acid and an ester prodrug, mycophenolate mofetil. *Immunol Rev* **1993**, *136*, 5-28, doi:10.1111/j.1600-065x.1993.tb00652.x.
36. Allison, A.C.; Kowalski, W.J.; Muller, C.D.; Eugui, E.M. Mechanisms of action of mycophenolic acid. *Ann N Y Acad Sci* **1993**, *696*, 63-87, doi:10.1111/j.1749-6632.1993.tb17143.x.
37. Pertwee, R.; Griffin, G.; Fernando, S.; Li, X.; Hill, A.; Makriyannis, A. AM630, a competitive cannabinoid receptor antagonist. *Life Sci* **1995**, *56*, 1949-1955, doi:10.1016/0024-3205(95)00175-6.

Preprints.org (www.preprints.org) | NOT PEER-REVIEWED | Posted: 22 April 2025 doi:10.20944/preprints202504.1842.v1

38. Hosohata, K.; Quock, R.M.; Hosohata, Y.; Burkey, T.H.; Makriyannis, A.; Consroe, P.; Roeske, W.R.; Yamamura, H.I. AM630 is a competitive cannabinoid receptor antagonist in the guinea pig brain. *Life Sci* **1997**, *61*, PL115-118, doi:10.1016/s0024-3205(97)00596-1.
39. Hosohata, Y.; Quock, R.M.; Hosohata, K.; Makriyannis, A.; Consroe, P.; Roeske, W.R.; Yamamura, H.I. AM630 antagonism of cannabinoid-stimulated [35S]GTP gamma S binding in the mouse brain. *Eur J Pharmacol* **1997**, *321*, R1-3, doi:10.1016/s0014-2999(97)00047-2.
40. Ross, R.A.; Brockie, H.C.; Stevenson, L.A.; Murphy, V.L.; Templeton, F.; Makriyannis, A.; Pertwee, R.G. Agonist-inverse agonist characterization at CB1 and CB2 cannabinoid receptors of L759633, L759656, and AM630. *Br J Pharmacol* **1999**, *126*, 665-672, doi:10.1038/sj.bjp.0702351.
41. Navarro, G.; Reyes-Resina, I.; Rivas-Santisteban, R.; Sánchez de Medina, V.; Morales, P.; Casano, S.; Ferreiro-Vera, C.; Lillo, A.; Aguinaga, D.; Jagerovic, N.; et al. Cannabidiol skews biased agonism at cannabinoid CB_1 and CB_2 receptors with smaller effect in CB1-CB2 heteroreceptor complexes. *Biochem Pharmacol* **2018**, *157*, 148-158, doi:10.1016/j.bcp.2018.08.046.
42. Thomas, A.; Baillie, G.L.; Phillips, A.M.; Razdan, R.K.; Ross, R.A.; Pertwee, R.G. Cannabidiol displays unexpectedly high potency as an antagonist of CB1 and CB2 receptor agonists in vitro. *Br J Pharmacol* **2007**, *150*, 613-623, doi:10.1038/sj.bjp.0707133.
43. Gado, F.; Ferrisi, R.; Polini, B.; Mohamed, K.A.; Ricardi, C.; Lucarini, E.; Carpi, S.; Domenichini, F.; Stevenson, L.A.; Rapposelli, S.; et al. Design, Synthesis, and Biological Activity of New CB2 Receptor Ligands: from Orthosteric and Allosteric Modulators to Dualsteric/Bitopic Ligands. *J Med Chem* **2022**, *65*, 9918-9938, doi:10.1021/acs.jmedchem.2c00582.
44. Ferrisi, R.; Polini, B.; Ricardi, C.; Gado, F.; Mohamed, K.A.; Baron, G.; Faiella, S.; Poli, G.; Rapposelli, S.; Saccomanni, G.; et al. New Insights into Bitopic Orthosteric/Allosteric Ligands of Cannabinoid Receptor Type 2. *Int J Mol Sci* **2023**, *24*, doi:10.3390/ijms24032135.
45. Huang, W.R.; Tu, J.X.; Qiao, A.Q.; Chen, L.J. GW842166X Alleviates Osteoarthritis by Repressing LPS-mediated Chondrocyte Catabolism in Mice. *Curr Med Sci* **2022**, *42*, 1046-1054, doi:10.1007/s11596-022-2627-z.
46. Liu, X.; Yu, H.; Chen, B.; Friedman, V.; Mu, L.; Kelly, T.J.; Ruiz-Pérez, G.; Zhao, L.; Bai, X.; Hillard, C.J.; et al. CB2 Agonist GW842166x Protected against 6-OHDA-Induced Anxiogenic- and Depressive-Related Behaviors in Mice. *Biomedicines* **2022**, *10*, doi:10.3390/biomedicines10081776.
47. Naikoo, R.A.; Painuli, R.; Akhter, Z.; Singh, P.P. Cannabinoid receptor 2 (CB2) modulators: A patent review (2016-2024). *Bioorg Chem* **2024**, *153*, 107775, doi:10.1016/j.bioorg.2024.107775.
48. Diaz, P.; Phatak, S.S.; Xu, J.; Fronczek, F.R.; Astruc-Diaz, F.; Thompson, C.M.; Cavasotto, C.N.; Naguib, M. 2,3-Dihydro-1-benzofuran derivatives as a series of potent selective cannabinoid receptor 2 agonists: design, synthesis, and binding mode prediction through ligand-steered modeling. *ChemMedChem* **2009**, *4*, 1615-1629, doi:10.1002/cmdc.200900226.
49. Xu, J.J.; Diaz, P.; Bie, B.; Astruc-Diaz, F.; Wu, J.; Yang, H.; Brown, D.L.; Naguib, M. Spinal gene expression profiling and pathways analysis of a CB2 agonist (MDA7)-targeted prevention of paclitaxel-induced neuropathy. *Neuroscience* **2014**, *260*, 185-194, doi:10.1016/j.neuroscience.2013.12.028.
50. Wu, J.; Hocevar, M.; Bie, B.; Foss, J.F.; Naguib, M. Cannabinoid Type 2 Receptor System Modulates Paclitaxel-Induced Microglial Dysregulation and Central Sensitization in Rats. *J Pain* **2019**, *20*, 501-514, doi:10.1016/j.jpain.2018.10.007.
51. Wu, J.; Bie, B.; Yang, H.; Xu, J.J.; Brown, D.L.; Naguib, M. Activation of the CB2 receptor system reverses amyloid-induced memory deficiency. *Neurobiol Aging* **2013**, *34*, 791-804, doi:10.1016/j.neurobiolaging.2012.06.011.
52. Wu, J.; Hocevar, M.; Foss, J.F.; Bie, B.; Naguib, M. Activation of CB_2 receptor system restores cognitive capacity and hippocampal Sox2 expression in a transgenic mouse model of Alzheimer's disease. *Eur J Pharmacol* **2017**, *811*, 12-20, doi:10.1016/j.ejphar.2017.05.044.
53. Xu, J.; Tang, Y.; Xie, M.; Bie, B.; Wu, J.; Yang, H.; Foss, J.F.; Yang, B.; Rosenquist, R.W.; Naguib, M. Activation of cannabinoid receptor 2 attenuates mechanical allodynia and neuroinflammatory responses in a chronic post-ischemic pain model of complex regional pain syndrome type I in rats. *Eur J Neurosci* **2016**, *44*, 3046-3055, doi:10.1111/ejn.13414.

Preprints.org (www.preprints.org) | NOT PEER-REVIEWED | Posted: 22 April 2025 doi:10.20944/preprints202504.1842.v1

54. Demuth, D.G.; Molleman, A. Cannabinoid signalling. *Life Sci* **2006**, *78*, 549-563, doi:10.1016/j.lfs.2005.05.055.
55. Soethoudt, M.; Grether, U.; Fingerle, J.; Grim, T.W.; Fezza, F.; de Petrocellis, L.; Ullmer, C.; Rothenhäusler, B.; Perret, C.; van Gils, N.; et al. Cannabinoid CB_2 receptor ligand profiling reveals biased signalling and off-target activity. *Nat Commun* **2017**, *8*, 13958, doi:10.1038/ncomms13958.
56. Howlett, A.C.; Abood, M.E. CB_1 and CB_2 Receptor Pharmacology. *Adv Pharmacol* **2017**, *80*, 169-206, doi:10.1016/bs.apha.2017.03.007.
57. Gasperi, V.; Guzzo, T.; Topai, A.; Gambacorta, N.; Ciriaco, F.; Nicolotti, O.; Maccarrone, M. Recent Advances on Type-2 Cannabinoid (CB_2) Receptor Agonists and their Therapeutic Potential. *Curr Med Chem* **2023**, *30*, 1420-1457, doi:10.2174/0929867329666220825161603.
58. Legare, C.A.; Raup-Konsavage, W.M.; Vrana, K.E. Therapeutic Potential of Cannabis, Cannabidiol, and Cannabinoid-Based Pharmaceuticals. *Pharmacology* **2022**, *107*, 131-149, doi:10.1159/000521683.
59. Zagzoog, A.; Brandt, A.L.; Black, T.; Kim, E.D.; Burkart, R.; Patel, M.; Jin, Z.; Nikolaeva, M.; Laprairie, R.B. Assessment of select synthetic cannabinoid receptor agonist bias and selectivity between the type 1 and type 2 cannabinoid receptor. *Sci Rep* **2021**, *11*, 10611, doi:10.1038/s41598-021-90167-w.
60. Sugiura, T.; Kondo, S.; Sukagawa, A.; Nakane, S.; Shinoda, A.; Itoh, K.; Yamashita, A.; Waku, K. 2-Arachidonoylglycerol: a possible endogenous cannabinoid receptor ligand in brain. *Biochem Biophys Res Commun* **1995**, *215*, 89-97, doi:10.1006/bbrc.1995.2437.
61. Yuan, J.; Yang, B.; Hou, G.; Xie, X.Q.; Feng, Z. Targeting the endocannabinoid system: Structural determinants and molecular mechanism of allosteric modulation. *Drug Discov Today* **2023**, *28*, 103615, doi:10.1016/j.drudis.2023.103615.
62. Aghazadeh Tabrizi, M.; Baraldi, P.G.; Borea, P.A.; Varani, K. Medicinal Chemistry, Pharmacology, and Potential Therapeutic Benefits of Cannabinoid CB2 Receptor Agonists. *Chem Rev* **2016**, *116*, 519-560, doi:10.1021/acs.chemrev.5b00411.
63. Nevalainen, T. Recent development of CB2 selective and peripheral CB1/CB2 cannabinoid receptor ligands. *Curr Med Chem* **2014**, *21*, 187-203, doi:10.2174/09298673113206660296.
64. Ishiguro, H.; Kibret, B.G.; Horiuchi, Y.; Onaivi, E.S. Potential Role of Cannabinoid Type 2 Receptors in Neuropsychiatric and Neurodegenerative Disorders. *Front Psychiatry* **2022**, *13*, 828895, doi:10.3389/fpsyt.2022.828895.
65. Kibret, B.G.; Ishiguro, H.; Horiuchi, Y.; Onaivi, E.S. New Insights and Potential Therapeutic Targeting of CB2 Cannabinoid Receptors in CNS Disorders. *Int J Mol Sci* **2022**, *23*, doi:10.3390/ijms23020975.
66. Legge, S.E.; Jones, H.J.; Kendall, K.M.; Pardiñas, A.F.; Menzies, G.; Bracher-Smith, M.; Escott-Price, V.; Rees, E.; Davis, K.A.S.; Hotopf, M.; et al. Association of Genetic Liability to Psychotic Experiences With Neuropsychotic Disorders and Traits. *JAMA Psychiatry* **2019**, *76*, 1256-1265, doi:10.1001/jamapsychiatry.2019.2508.
67. Ishiguro, H.; Horiuchi, Y.; Ishikawa, M.; Koga, M.; Imai, K.; Suzuki, Y.; Morikawa, M.; Inada, T.; Watanabe, Y.; Takahashi, M.; et al. Brain cannabinoid CB2 receptor in schizophrenia. *Biol Psychiatry* **2010**, *67*, 974-982, doi:10.1016/j.biopsych.2009.09.024.
68. Naguib, M.; Xu, J.J.; Diaz, P.; Brown, D.L.; Cogdell, D.; Bie, B.; Hu, J.; Craig, S.; Hittelman, W.N. Prevention of paclitaxel-induced neuropathy through activation of the central cannabinoid type 2 receptor system. *Anesth Analg* **2012**, *114*, 1104-1120, doi:10.1213/ANE.0b013e31824b0191.

Disclaimer/Publisher's Note: The statements, opinions and data contained in all publications are solely those of the individual author(s) and contributor(s) and not of MDPI and/or the editor(s). MDPI and/or the editor(s) disclaim responsibility for any injury to people or property resulting from any ideas, methods, instructions or products referred to in the content.